

Microstructural Analysis of AgIn_5VI_8 (VI: S, Se, Te) Ternary Semiconductors by X-Ray Diffraction

José R. Fermin^{a,b,*} , Carlos Durante Rincón^a, Jaime A. Castro^a

^aDepartamento de Física, Facultad Experimental de Ciencias, Universidad del Zulia, Maracaibo, Venezuela.

^bFacultad de Ingeniería, Universidad Rafael Urdaneta, Maracaibo, Venezuela.

Received: November 23, 2018; Revised: August 07, 2019; Accepted: September 18, 2019

This work is a study of the microstructural properties of the polycrystalline ternary compounds AgIn_5S_8 , AgIn_5Se_8 , and AgIn_5Te_8 by X-ray diffraction technique (XRD). The full-width-half-maximum (FWHM) of the XRD profile is measured as function of the diffraction angle and used to estimate the microstructural parameters. In general, a microstructural characterization by XRD is principally performed by Strain/Size analysis based on the modified Scherrer formula, which in turn, allows for mean grain size and average microstrain to be computed. However, when applied to polycrystalline bulk semiconductors, the modified Scherrer formula gives grain sizes of the order of a few hundreds of nanometers, which is not usually observed in bulk materials. Instead, a new theoretical scheme with misfit dislocations and plastic deformations would be used to calculate the grain size into a bulk. Assuming that these dislocations are of elastic origin, we were able to calculate the misfit dislocations density as function of the elastic constants of the materials. With this, the modified Scherrer formula is corrected to explain the additional XRD line broadening. All microstructure parameters of our samples increase as the atomic radius of the VI-element increases, with elastic constants similar to related semiconducting compounds.

Keywords: Strain/Size analysis, Modified Scherrer Equation, microstructural parameters, ternary semiconductors AgIn_5VI_8 , Poisson ratio.

1. Introduction

Ternary semiconductors provide a natural way of tuning the desired band gap and flexibility to control other material parameters by changing the relative composition of the pure elements in the alloy. A special group of ternaries are those based on the groups of elements I-III-VI, such as $\text{Ag}(\text{In}, \text{Ga})$ (S, Te, Se), CuInSe_2 and AgGaTe_2 .¹⁻³ These alloys crystallize in the non-centrosymmetric chalcopyrite structure, leading to non-zero second order nonlinear susceptibility. This gives these compounds promising features for technological applications, including infrared optoelectronic devices and solar cells applications.^{4,5} Another group of semiconductors that have gained much attention during recent years are those from the family of I-III₅-VI₈ compounds.⁶⁻⁸ These alloys present a tetragonal or orthorhombic structure depending on the ion of group III, and a cubic-spinel or tetragonal structure depending on the group VI element,⁷ and have optical band gaps suitable for optimum energy conversion solar cells, and thermoelectric properties useful for applications in waste-heat recovery, air conditioning, and refrigeration.

The optical and thermal properties of semiconductor materials are closely related to morphology and grain size.⁹ Understanding this relationship is critically important to many industrial processes. Furthermore, the physical properties of the semiconductor elements involved in the design of microelectronic devices are highly dependent on their microstructural parameters, such as degree of crystallinity, crystallographic orientation, grain size, elastic/plastic deformation, etc.¹⁰ Among the various experimental methods used for determination of the microstructural parameters in polycrystalline solids, X-ray diffraction (XRD)-based techniques play an important role in materials science.¹¹ This is because the XRD patterns are very sensitive to the crystallographic structure and orientation, phase changes, structural defects, chemical composition, etc., which are essential in the interpretation of the physical data. On the other hand, any XRD measurement must be followed by a theoretical analysis method in order to provide a suitable interpretation of the diffraction spectra, and this turns into an essential issue in materials science research. The most widely-used method in microstructural analysis in bulk

*e-mail: jfermin70@gmail.com

materials is the Strain/Size method.¹² This technique for analysis is based on the interpretation of the broadening of the diffraction lines on the framework of the Scherrer equation,¹³ from which, microstructural parameters, such as grain size and average microstrain, are determined. It is apparent that these two parameters are the most relevant in the description of a microstructure; however, when an actual sample is subjected to strain forces, structural defects must be introduced in order to stabilize the crystalline lattice. These structural defects are called misfit dislocations and contribute to an extra broadening in the experimental full-width at half-maximum (FWHM) of the XRD lines. These defects are not usually taken into account in a conventional microstructural analysis based on the Scherrer equation, so some corrections are needed in order to provide a more realistic description of a microstructure.

2. Experimental Methods

Three polycrystalline ingots of AgIn_3S_8 , AgIn_3Se_8 , and AgIn_3Te_8 were prepared by direct fusion of the stoichiometric mixture (DFSM) of the elements of at least 5N purity, following a synthesis program similar to that outlined by Pérez et al.¹³ The samples were synthesized inside evacuated quartz ampoules ($\approx 10^{-6}$ Torr). The ampoules were very slowly heated in a vertical furnace, from room temperature up to 858 °C at a heating rate of about 5 °C/h, lower enough to prevent an explosion due to exothermic reactions between group III and group VI elements. The samples are kept at this temperature during 48 hours, and rocked at regular intervals to achieve a homogeneous mixing of the liquid phase of the reacting mixture, and then cooled at the same rate of 5 °C/h. At such slow cooling rate the formation of undesirable phases is also prevented.

The X-ray diffraction patterns were performed using a Bruker D8 Focus powder diffractometer with the $\text{CuK}\alpha_1$ characteristic line (1.5405 Å), and in the Bragg-Brentano geometry. The diffraction patterns were collected in the range $5^\circ \leq 2\theta \leq 100^\circ$, with a step size of 0.02, and a step time of 15.0 sec. The diffraction spectra were indexed by using the WINPLOTR/TREOR 90 graphic interface, and the lattice parameters were then calculated. The microstructural parameters of the samples were determined from the full-width-half-maximum (FWHM) of their XRD profiles, using a Strain/Size analysis method based on a theoretical model which will subsequently be described in more detail.

3. Theoretical Considerations

3.1 The Modified Scherrer Equation

The microstructural analysis by XRD of solid materials is based on the calculation of certain physical parameters, such as grain size, strain forces, crystalline materials dislocations,

and elastic moduli. In general, the grain is a composite of several crystallites made-up of unit cells, and is often related to the full-width-half-maximum (FWHM) of the diffraction pattern, by means of the well-known Scherrer equation.¹⁴

$$\beta_L = \frac{K\lambda}{L \cos \theta}. \quad (1)$$

where β_L is the FWHM in radians; $K=2[\ln(2)/\pi]^{1/2}$ is a constant related to the grain shape, and is of the order of ≈ 0.93 for spherical grains; λ is the X-ray wavelength in Å, L the average size of the grain/crystallite in Å, and θ the Bragg angle in degrees. The Scherrer formula is useful when the grain/crystallite size is considered to be primarily responsible for the broadening of XRD peaks and predicts real L -values in the case when the grain and crystallite sizes are similar. The limit of application of Scherrer Equation stills a matter of discussion, and in fact some authors set this limit below 100 nm,¹⁵ while some others argue that it is only valid for grain sizes less than 200 nm.¹³ More recently, Muniz et al.¹⁶ establish a criterion according to which, the limit of applicability of the Scherrer Equation depends on the crystalline reflections and on the XRD absorption.

In a polycrystalline sample, the assumption that the crystallite size matches the grain size is not always valid. In these materials, grains are made up of small crystallites oriented in all directions. In this case, the size effects could be overwhelmed by an anisotropic microstructure, characterized by the presence of microstrains between atomic planes. In order to stabilize the grain size, the microstrains must be compensated by local elastic forces, as a consequence inducing misfit dislocations and mosaicities, deformations, stacking faults, vacancies, composition gradients, etc. Due to this relaxation process, the lines of the XRD profile display an additional broadening, represented by the expression,¹⁷

$$\beta_\varepsilon = 4\varepsilon \tan \theta. \quad (2)$$

where $\varepsilon = (d' - d)/d$ is the microstrain between crystalline planes and is a measure of the elastic deformation; d and d' are the interplanar distances before and after deformation, respectively. Another aspect to be considered in our analysis is the aberration introduced by the diffractometer to the FWHM, or instrumental broadening, β_{inst} . The instrumental broadening is parameterized from a reference silicon data using the Caglioti's formula,¹⁸

$$\beta_{inst}^2 = U \tan^2 \theta + V \tan \theta + W. \quad (3)$$

where U , V and W are fitting parameters to the base XRD-line. In our case, $U = 0.000010$, $V = 0.0000015$, and

$W = 0.0000055$. With this, the $FWHM$, $\beta(\theta)$, relates to microstructure parameters through the direct sum of each contribution¹⁹

$$\beta(\theta) = \frac{K\lambda}{L \cos \theta} + 4\epsilon \tan \theta + \beta_{inst}. \quad (4)$$

Eq. (4) is often used when the profile of the diffraction line corresponds to a Lorentzian function. These profiles are typically observed when the micro-deformations field is isotropic, and size effects overwhelm the microstrains distribution. In the case of many polycrystalline solids the deformation field is anisotropic, however, contributing to the line broadening with a Gaussian profile, and with $FWHM$ given by the quadratic expression²⁰

$$\beta^2(\theta) = \left(\frac{K\lambda}{L \cos \theta} \right)^2 + (4\epsilon \tan \theta)^2 + \beta_{inst}^2. \quad (5)$$

Expressions (4) and (5) are known as the modified Scherrer formulae and are the fundamental basis for the Strain/Size analysis by XRD in solid materials. In general, in polycrystalline materials with low crystallinity, the profile of the XRD spectrum corresponds to a linear combination of a Lorentzian line to a Gaussian line, making the $FWHM$ analysis rather complicated. The microstructural parameters L and ϵ are determined from least square fits with Eqs. (4) or (5), according to the case. The L -values predicted by the modified Scherrer Equations are still of the order of some hundreds of nm, which are in most cases unrealistic in the case of bulk polycrystalline materials. This is because as the polycrystalline sample approaches the bulk, grain sizes of the order of a few microns are observed. In this range of sizes, the density of lattice dislocations increases and must be explicitly taken into account, introducing an additional line broadening given by $\beta_D^2 = 9b^2\rho_D$,²¹ where ρ_D is the misfit dislocation density per unit area, and b is the module of the Burger vector which defines the direction of the dislocations line perpendicular to the hkl plane. The problem now becomes finding an analytical expression for the function ρ_D . This is not an easy task, since the structure of a dislocation line is in general very complex. However, since the lattice dislocations are strictly elastic in origin, the problem reduces to calculation of the dislocation density at mechanical equilibrium, as will be shown in the following section.

3.2 Elastic Relaxation. Mechanical Properties

The problem of elastic relaxation in semiconductors has been a subject of great interest during the past decades.²² This is because strain/stress forces give adequate information regarding materials' elastic constant, and in turn, provide

a way to control the mechanical properties. Intuitively, at equilibrium, the energy of elastic forces along dislocation lines must satisfy the condition $E_{el} = E_D$, with E_{el} and E_D being the strain energy density and the energy density stored by misfit dislocations, respectively. This is a necessary condition for mechanical stabilization of the material, and it is useful in the study of elastic properties, as will be shown in greater detail. The energy density of elastic deformations is given by (within the Hooke's law approximation)

$$E_{el} = \frac{1}{2} B \epsilon^2. \quad (6)$$

where ϵ is the average microstrain, and B is the bulk modulus related to the elastic constants of the material, which are,²³

$$\begin{aligned} C_{11}, C_{12}, C_{44} & : \text{cubic}, \\ C_{11}, C_{12}, C_{13}, C_{44} & : \text{hexagonal}, \\ C_{11}, C_{12}, C_{13}, C_{33}, C_{44}, C_{66} & : \text{tetragonal}. \end{aligned} \quad (7)$$

In particular, for a single cubic crystal $B = (C_{11} + 2C_{12})/3$. As mentioned above, accurate calculations of the misfit dislocations energy are further complicated, since a dislocation line is a complex structure. In the usual case the energy of an array of dislocations is the elastic energy stored within the dislocation line. If the strain field is distributed along screw and edge dislocations, the misfit dislocation energy density is calculated following the model discussed by Sutton and Balluffi.²⁴ It is then obtained that,

$$dE_D(\phi) = \frac{d\phi}{4\pi(1-\nu)} \mu b^2 \rho_D \ln\left(\frac{L}{b}\right) (1 + \nu \cos^2 \phi). \quad (8)$$

with μ being the effective shear modulus, ν the Poisson ratio, L the size of a grain/crystallite intercepting a dislocation line, b the modulus of the corresponding Burger vector, ρ_D the misfit dislocation density per unit area, and ϕ the angle between the Burger vector and the dislocation line, in the range from 0 (screw) to $\pi/2$ (edge). The Poisson ratio gives information on the material's plasticity and is defined as the negative ratio "transversal-strain/longitudinal-strain" for the unit cell ($-1 < \nu < 0.5$). Most semiconductors exhibit positive ν -values, which indicate that when subjected to a strain force the material elongates longitudinally, while it is compressed transversally. In contrast, there are certain special man-made materials that can exhibit a negative Poisson's ratio and are called "auxetic". In order for any solid structure be stable, elastic energy must be absorbed in the same amount along each crystalline direction. Integrating Eq. (8) gives the total energy density due to misfit dislocations as,

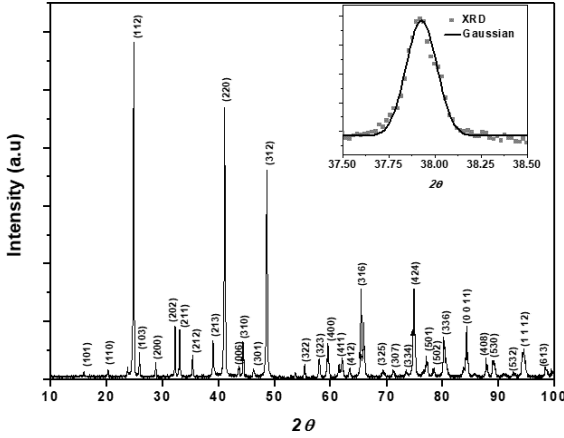


Figure 3. Profile of the XRD spectrum of the compound AgIn_5Te_8 . The lineshape of the diffraction peaks fit in general to a Gaussian profile, as observed from the inserted figure.

been reported in related semiconducting compounds such as $\text{AgIn}_4\text{GaTe}_8$.¹⁶ Notice that the θ_c value coincides with the strongest reflection peak, with a shift from $\cong 13.65^\circ$ to $\cong 12.39^\circ$ as the atomic number, z , of the anion VI increases from 16 up to 54. This shift can be understood considering Bragg's law, $\sin\theta_c = \lambda/2d(z)$, from which we can verify that the interplanar distance calculated at θ_c satisfies the inequality $d(\text{S}) < d(\text{Se}) < d(\text{Te})$. The continuous curves in Fig. 4 are non-linear numerical fits to the experimental data using Eq. (13), following a Levenberg-Marquardt scheme.²⁸ The values of the parameters obtained from these fits are listed in Table 1. The agreement between theory and experiment is good for the set of parameters (L , ε , ν), satisfying the theoretical conditions discussed in section 3.2. Notice that both grain size and microstrain increase along with the atomic number of the anion VI, with increasing Poisson ratio. This means that our samples are highly anisotropic with the Poisson ratio typical of other related ternaries.²⁹ The grain sizes obtained with our model are of the order of a few microns, which is reasonable in bulk polycrystalline materials.^{30,31}

By comparison, the curves obtained from the Scherrer (S) and the Modified Scherrer (MS) equations are also shown in Fig.4. Notice that the agreement between experimental data and the MS equation is also reasonable for the corresponding pair of parameters (L_{MS} , ε_{MS}) listed in Table 1. Although the average microstrain, ε_{MS} is comparable to the value of ε , the grain size, L_{MS} is of the order of ≈ 250 nm. However, as mentioned before, such small grain sizes are not usually observed in bulk polycrystalline materials. On the other hand, the conventional Scherrer formula (1), can only fit the experimental line broadening at diffraction angles smaller than θ_c and departs from the experimental data at diffraction angles $\theta > \theta_c$, giving much smaller grain sizes of the order of ≈ 50 nm.

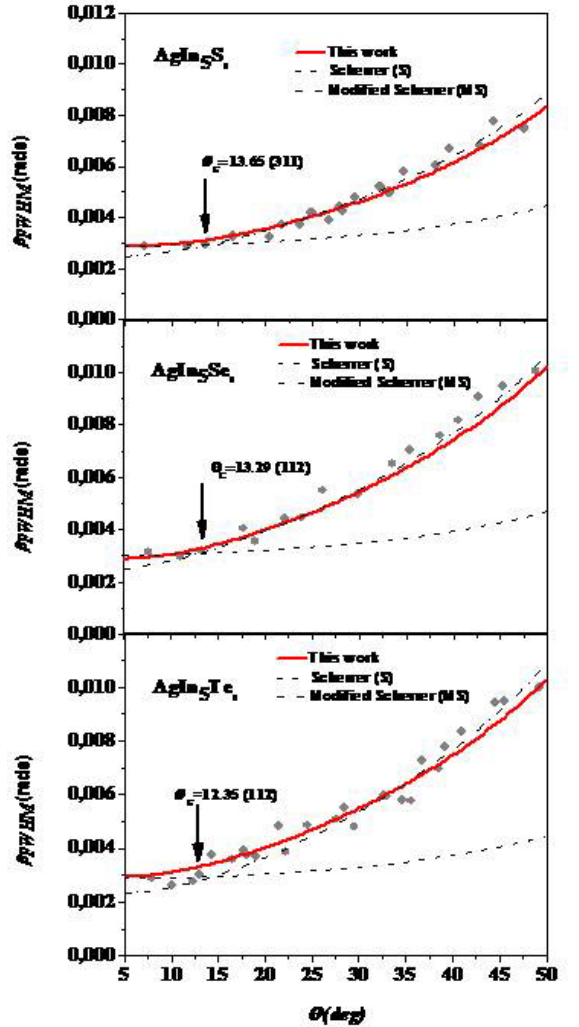


Figure 4. Full-Width-Half-Maximum (β_{FWHM}) as function of the diffraction angle for each sample. The solid curves are numerical fits of the experimental data using equation (13). The fitting parameters obtained from these fits are listed in Table 1. The dashed-dotted curve is calculated with the modified Scherrer formula (5), and the dashed curve corresponds to the conventional Scherrer formula.

Table 1. Microstructural parameters (L, ε, ν) of the system AgIn_5VI_8 determined from numerical fits with Equation (13), as discussed in Section 4. For comparison, the parameters obtained from the modified Scherrer (MS) and conventional Scherrer (S) formulae are also included.

	AgIn_5S_8	AgIn_5Se_8	AgIn_5Te_8
L (μm)	1.56	5.51	8.51
ε (%)	0.17	0.21	0.28
ν	0.125	0.23	0.30
L_{MS} (nm)	245.0	258.0	262.0
ε_{MS} (%)	0.15	0.22	0.24
L_S (nm)	48.0	46.0	50.5

5. Conclusions

The microstructural properties of polycrystalline semiconductors AgIn_5VI_8 (VI=S, Se, Te) are studied applying the Strain/Size method to the Full-Width-Half-Maximum of the x-ray diffraction profiles. From our analysis we can conclude:

1. The FWHM of the diffraction line as a function of θ cannot be explained by the modified Scherrer formulae in their original forms, since these give in most cases unrealistic grain sizes for a polycrystalline sample.
2. In order to give a more realistic interpretation of the FWHM, misfit dislocations must be included explicitly. In this framework, plastic deformations are important. The Poisson ration, ν , then appears as a fundamental microstructural parameter beside the mean grain size, L , and the average microstrain, ε . In this way, the modified Scherrer formulae are then corrected with an additional line broadening, β_D .
3. The values of the microstructural parameters (L , ε , ν) for the ternary system AgIn_5VI_8 depend on the atomic radius of the VI element. In particular, according to our model, the Poisson ration is positive in all samples and of the same order than those found in related semiconducting materials, which indicate that all these semiconductors have similar mechanical properties.

The detection and quantification of microstrains and microstructural defects in polycrystalline compounds and granular systems are, in general, complex tasks, since several parameters are involved, requiring highly sensitive techniques and more fundamental theoretical studies. However, the results reported here could be of relevance for future applications of AgIn_5VI_8 in diverse semiconducting processes and microelectronic devices.

6. Acknowledgements

The Authors wish to thank the agencies Consejo de Desarrollo Científico y Humanístico-LUZ (CONDES) (CC-0595-10), and FONACIT (201100542) by their financial support. At the same time we also thank the staff of the Centro Nacional de DRX (ULA) for technical support in the XRD measurements.

7. References

1. Delgado GE, Mora AJ. Structural characterization of the semiconductor chalcogenide system Ag-In-VI (VI=S, Se, Te) by X-ray powder diffraction. *Chalcogenide Letters*. 2009;51:635-639.
2. Zhang SB, Wei S, Zunger A. Stabilization of Ternary Compounds via Ordered Arrays of Defect Pairs. *Physical Review Letters*. 1997;78(21):4059.
3. Burger A, et al. Preparation and thermophysical properties of AgGaTe_2 crystals. *Journal of Crystal Growth*. 2001;225(2-4):505-511.
4. Matsushita H, Takashi M, Katsui A, Takizawa T. Thermal analysis and synthesis from the melts of Cu-based quaternary compounds Cu-III-IV-VI₄ and Cu₂-II-IV-VI₄ (II=Zn, Cd; III=Ga, In; IV=Ge, Sn; VI=Se). *Journal of Crystal Growth*. 2000;208(1-4):416-422.
5. Krustok J, Jagomägi A, Grossberg M, Raudoja J, Danilson M. Photoluminescence properties of polycrystalline AgGaTe_2 . *Solar Energy Materials & Solar Cells*. 2006;90:1973-1982.
6. Sánchez A, et al. Structural, optical, and electrical properties of AgIn_5Te_8 . *Journal of Applied Physics*. 2005;97(5):053505-4.
7. Charoenphakdee A, Kurosaki K, Muta H, Uno M, Yamanaka S. Thermal conductivity of the ternary compounds: AgMTe_2 and AgM_5Te_8 (M = Ga or In). *Materials Transactions*. 2009;50(7):1603-1606.
8. Rincón CAD, Durán LT, Medina JE, Castro JA, León M, Fermin JR. Structural and optical properties of AgIn_5S_8 . *International Journal of Modern Physics B*. 2017;31(31):1750246-10.
9. Kalihari V, Tadmor EB, Haugstad G, Frisbie CD. Grain Orientation Mapping of Polycrystalline Organic Semiconductor Films by Transverse Shear Microscopy. *Advanced Materials*. 2008;20(21):4033-4039.
10. de Wit R. Elastic Constants and Thermal Expansion Averages of a Nontextured Polycrystal. *Journal of Mechanics and Structures*. 2008;3(2):193-212.
11. Warren BE. *X-Ray Diffraction*. Massachusetts: Addison-Wesley Pub. Co.; 1969.
12. Mittemeijer EJ, Welzel U. The "state of the art" of the diffraction analysis of crystallite size and lattice strain. *Zeitschrift für Kristallographie*. 2008;223:552-560.
13. Pérez FV, Gando NJ, Castro JÁ, Rincón CAD, Durán L, Fermin JR. Structural properties of and morphology of the quaternary semiconductor $\text{AgIn}_4\text{GaTe}_8$. *Journal of Material Sciences & Engineering*. 2015;4(1):1-4.
14. Patterson AL. The Scherrer Formula for X-Ray Particle Size Determination. *Physical Review*. 1939;56:978.
15. Monshi A, Foruoghi MR, Monshi MR. Modified Scherrer Equation to Estimate More Accurately Nano-Crystallite Size Using XRD. *World Journal of Nano Science and Engineering*. 2012;2(3):154-160.
16. Muniz FTL, Miranda MA, Santos CM, Sasaki JM. The Scherrer equation and the dynamical theory of X-ray diffraction. *Acta Crystallographica. Section A, Foundations and Advances*. 2016;72(Pt 3):385-390.
17. Danilchenko S, Kukharenko OG, Moseke C, Protsenko IY, Sukhodub LF, Sulkio-Cleff B. Determination of the Bone Mineral Crystallite Size and Lattice Strain from Diffraction Line Broadening. *Crystal Research and Technology*. 2002;37(11):1234-1240.
18. Caglioti G, Paoletti A, Ricci FP. On resolution and luminosity of a neutron diffraction spectrometer for single crystal analysis. *Nucl Instrum Methods*. 1960;9(2):195-198.

19. Pavel K, Woodward PM. Liquid-Mix Disorder in Crystalline Solids: ScMnO_3 . *Journal of Solid State Chemistry*. 1998;141(1):78-88.
20. Balzar D, Popovic DS. Advances in X-ray Analysis. *Journal of Applied Crystallography*. 1996;29:16-23.
21. Yazici R, Kalyon D. Microstrain and defect analysis of CL-20 crystals by novel methods. *Journal of Energetic Materials*. 2005;23(1):43-58.
22. Matthews JW, Mader S, Light TB. Accomodation of misfit across the interface between crystals of semiconducting elements or compounds. *Journal of Applied Physics*. 1970;41(9):3800-3804.
23. Nye JF. *Physical properties of crystals*. London: Oxford University Press; 1957.
24. Sutton AP, Balluffi RW. *Interfaces in crystalline materials*. Oxford: Oxford Science Publications; 1995. v. 51.
25. Den Toonder JMJ, Van Dommelen JAW, Baaijens FPT. The relation between single crystal elasticity and the effective elastic behavior of polycrystalline materials: theory, measurement and computation. *Modelling and Simulation in Materials Science and Engineering*. 1999;7(6):909-928.
26. Medina JE, Durán LT, Castro J, Fermín JR, Hernández J, Rincón CAD. Structural and optical properties of AgIn_3Se_8 . *Materials Science: An Indian Journal*. 2015;12(5):178-184.
27. Sánchez A, Meléndez L, Castro J, Hernández JA, Hernández E, Rincón CAD. Structural, optical, and electrical properties of AgIn_3Te_8 . *Journal of Applied Physics*. 2005;97(5):053505.
28. Vetterling WT, Teukolsky SA, Press WH, Flannery BP. *Numerical Recipes*. 2nd ed. Cambridge: Cambridge University Press; 1992.
29. Martínez AM, Soriano R, Faccio R, Trigubó AB. Mechanical Properties Calculation of II-VI Semiconductors: $\text{Cd}_{1-y}\text{Zn}_y\text{Te}$ ($0 \leq y \leq 1$). *Procedia Materials Science*. 2015;8:656-664.
30. Berbenni S, Favier V, Berveiller M. Impact of the grain size distribution on the yield stress of heterogeneous materials. *International Journal of Plasticity*. 2007;23(1):114-142.
31. He Y, Winnubst L, Burggraaf AJ, Verweij H, Van der Varst PG, With B. Grain-Size Dependence of Sliding Wear in Tetragonal Zirconia Polycrystals. *Journal of the American Ceramic Society*. 1996;79(12):3090-96.